SEMI-AUTOMATED DESIGN OF MICROSTRIP DUAL BAND COAXIAL FEED ANTENNA USING DIFFERENTIAL EVOLUTION ALGORITHM FOR WLAN APPLICATIONS

Nguyen Thanh Huong*, Nguyen Van Thang

Abstract: *Traditional antenna design uses discrete steps manually to create and optimize the antenna structure. This approach costs both time and effort, especially when a complex antenna structure is on demand. The evolutionary algorithm emerges as a potential alternative method to formulate the antenna model as well as to optimize the structure so as to comply with the design requirements. In this paper, we propose a method for determining the surrogate model and dimensions of an ultra-wideband patch antenna using a differential evolution algorithm. This antenna is desired to work at the frequency range of 2.45GHz to 5.8GHz for WLAN applications. Through the evaluation of reflectivity and investigation of the algorithm,the surrogate model is obtained faster with optimized dimensions. The algorithm is investigated with different strategies to detect the best strategy when an object is a differential evolution applied.*

Keywords: Evolutionary algorithm; Differential evolution; Multiband antenna; Coaxial feed.

1. INTRODUCTION

With the rapid development of modern mobile/wireless communications, the need for a multiband antenna has gained much attention since it is more practical for a single system to support multiple communication standards simultaneously [1]. In the past, the microstrip antennas for Wi-Fi communication have been designed as dual-band antenna at 2.45GHz and 5.2GHz [3-6] or 2.45GHz and 5.8GHz [7-10]. Nowadays,the evolution algorithm is becoming increasingly popular in engineering design activity primarily because of the availability and affordability of high-speed computers. They are extensively used in those engineering design problems where the emphasis is on maximizing or minimizing a specific goal. Such algorithms include the Genetic Algorithm (GA). One paper presents the optimization of the notch band in an Ultra-Wide Band (3.1GHz to 10.6GHz and reject interference with existing wireless networking technologies such as IEEE802.11a in the U.S. (5.15-5.35GHz, 5.725-5.825GHz) and HIPERLAN/2 in Europe (5.15-5.35GHz, 5.47-5.725GHz)) serrated monopole antenna using a modified GA approach [11]. Several other evolution algorithms have also been applied for optimizing antennas. A letter presents the design of a planar antenna for ultrawideband (UWB) applications with a bandwidth of 5.5GHz over 3.7 to 9.2GHz and return loss values lower than 10dB and using particle swarm optimization with five control points have been used for the antenna description [12]. Another design of a probe-fed microstrip antenna is accomplished using a differential evolution algorithm and studied the effect of matching over the frequency range 2.38-2.42 GHz [13].

From the previously studied antenna research papers, it can be seen that mechanical design with an efficient algorithm is urgently needed for antenna design problems. This solution can fast tune the design and analysis of modern communication components to meet the requirements of compactness, bandwidth, reconfigurability, gain, directivity, etc. Thanks to these techniques, antenna parameters keep on changing without antenna design obstacles,heavy calculation, and time-consuming since parameters have to be computed using simultaneous analysis and design iteration. In this paper, we applied the DE algorithm, which is often applied to the problem with floating-point variables, to reach the smallest value to design a multi ultra-wideband antenna. Because of the popularity of dual ultra-wideband antenna that could be operated in WLAN and WIFI frequency bands, it is chosen for our design based on Coplanar Waveguide (CPW) fed feeding. In this paper, the differential evolution optimization algorithm is considered to minimize the reflection coefficient in the UWB frequency range by determining the appropriate antenna dimensions.The antenna is analyzed and optimized completely using CST Microwave Studio, and then the CST program is linked with the (DE) algorithm using a MATLAB program to optimize the antenna. Interchanging information between CST Microwave studio and MATLAB allows the implementation of mathematical or optimization algorithms and graphical possibilities, which is not included in the CST Microwave studio environment.

This article is organized as follows. Section 2 presents the basic principle of the Differential Evolution algorithm. In Section 3, the antenna structure is proposed and described. Based on the DE and the antenna geometry, the application of the algorithm to the optimization process is analyzed in Section 4. Section 5 demonstrates the achieved results for antenna simulation and measurement results after DE optimization. The last section draws a conclusion on the introduced approach.

2. FORMULATION OF DIFFERENTIAL EVOLUTION ALGORITHM

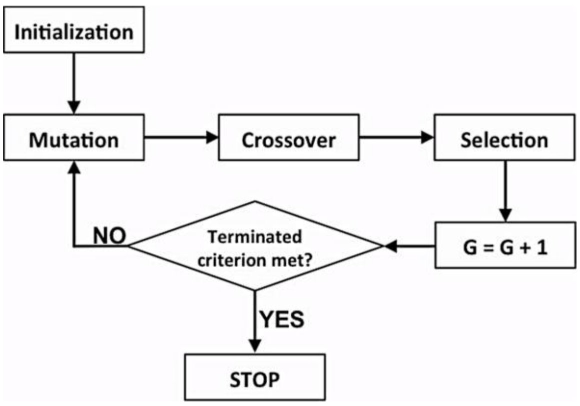

Figure 1. *Flow chart of the differential evolution algorithm.*

Differential evolution (DE) is a population-based, derivative-free function optimizer and was first introduced by Storn and Price in 1996 [14]. It usually encodes decision variables as floating-point numbers and manipulates them with simple arithmetic operations such as addition, subtraction, and multiplication. This algorithm obeys the law of evolutionary algorithms in which the significant differences are assessed during the mutation and selection process. Therefore, this DE algorithm depends on two parameters, the mutation factor or the so-called differential amplification factor (F) and the crossover probability (CR).The basic idea is to use vector differences by picking up randomly chosen vectors, then compute their difference as a way to interfere with the parent vector with an abnormal operator and probe the search space. Some variations of DE have been studied [15-16]; however, the critical principle usually concentrates on the nominal approach (DE/rand/1/bin). Each individual of the population encounters mutation and crossover, but when the crossover occurs, the offspring are compared to the parent in order to evaluate the fitness value (or terminated criterion). If the condition is satisfied, the next generation (selection) can continue. This DE process is displayed in figure 1.

In a standard DE algorithm, a feasible solution set is randomly created within search space. NP is the size of the solution set, and D is the dimension of the problem. The objective function values of NP solutions are evaluated based on the minimization condition. The main steps in the differential evolution algorithm are briefly outlined as followed:

Step 1: Initialization

Define an initial population of trial vectors. It is randomly generated according to a standard or uniform distribution.

$$\left\{ X_{1,j,0} = \left(x_{1,j,0}, x_{2,j,0}, x_{3,j,0}, \ldots, x_{D,j,0} \right) \middle| j = 1, 2, 3, \ldots, NP \right\} \tag{1}$$

Each trial vector contains different parameters of the design. For each parameter, a lower limit and an upper limit are defined:

$$x_i^{low} \le x_{i,j,0} \le x_i^{up} \,\middle|\, i = 1, 2, 3, \ldots, D \tag{2}$$

After initialization, DE performs aloop of evolutionary operations: mutation, crossover, and selection.

Step 2: Mutation

At each generation g, this operation creates mutation vectors $v_{j,g}$ based on the current parent population. Mutation strategies used in the paper:

DE/rand/1: $v_{j,g} = X_{r0,g} + F \times \left(X_{r1,g} - X_{r2,g} \right)$ (3)

DE/current-to-rest/1: $v_{j,g} = X_{r0,g} + F \times \left(X_{best,g} - X_{r2,g} \right) + F \times \left(X_{r1,g} - X_{r2,g} \right)$ (4)

DE/best/1: $v_{j,g} = X_{best,g} + F \times \left(X_{r1,g} - X_{r2,g} \right)$ (5)

RDE: $v_{j,g} = X_{r1,g} + F \times \left(X_{best,g} - X_{r2,g} \right) + \left(1 - F \right) \times \left(X_{best,g} - X_{r3,g} \right)$ (6)

The scaling factor F scales the difference between two vectors and adds it to the third vector, which ranges from 0 to 1. $X_{best,g}$ is the best vector at the current generation.

Step 3: Crossover

After mutation, a 'binomial' crossover operation forms the final trial vector.

$$u_{j,g} = \left(u_{1,j,g}, u_{2,j,g}, \ldots, u_{D,j,g} \right)$$

$$u_{i,j,g} = \begin{cases} v_{i,j,g} \ldots \; if\ rand_i \left(0,1 \right) \le CR\ or\ i = i_{rand} \\ x_{i,j,g} \qquad otherwise \end{cases}$$

$i_{rand} = i_{randient}(1, D)$ is the integer randomly chosen from 1 to D and newly generated for each i, the cross over probability, $CR \in [0,1]$, roughly corresponds to the average fraction of vector components that are inherited from the mutation vector.

Step 4: Selection

The trial vector is compared with the corresponding its counterpart in the current population, and the one with better fitness is admitted to the next generation.

$$X_{j,g+1} = \begin{cases} u_{j,g} & \text{if } f(u_{j,g}) \le f(X_{j,g}) \\ X_{j,g} & \text{otherwise} \end{cases}$$

In differential evolution, crossover probability CR discussed above is taken to be 0.5. Out of various schemes available, the version of DE chosen is DE/rand/1, where the scaling factor F is a random number between 0-1 generated by MATLAB at each generation of the algorithm. Ultimately, all of the individuals of the next generation are as good as or better than their counterparts in the current generation.The steps to the semi-automatic design of a PIFA antenna using the differential evolution algorithm are discussed in more detail in section 4.

3. ANTENNA STRUCTURE DESIGN

Wireless communication has progressed rapidly in recent years, and many mobile units are getting smaller. In order to meet the requirement of miniaturization, the antennas used in mobile terminals must be reduced in size accordingly. Planar antennas, such as microstrip and printed antennas, have attractive features such as low profile, small size, and suitability for server mounting and are an up-and-coming candidate to meet design considerations. Among planar antennas, the Planar Inverted-F antenna (PIFA) is increasingly used in the mobile phone market. It resonates at a quarter-wavelength, thus, reducing the required space needed, and typically has a low profile, omnidirectional pattern, and good SAR properties. This antenna resembles an inverted F, which is shown in fig. 2a.

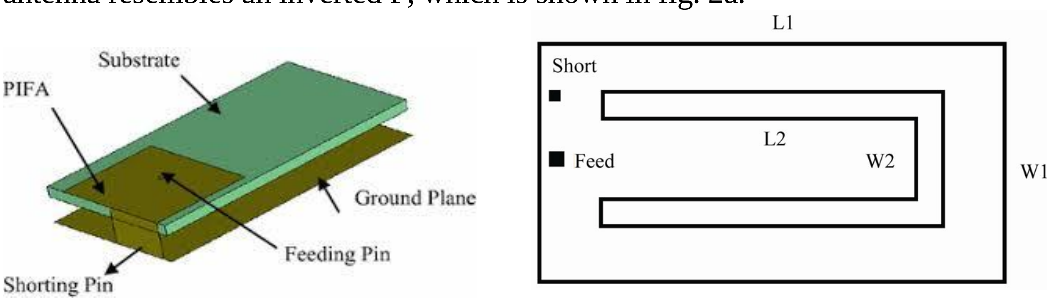

a) b)

Figure 2.*a) Configuration of the PIFA antenna;*

b) Radiating surface of PIFA antenna

PIFA consists of a unipolar antenna that runs parallel to the ground plane and is grounded at one end, and is powered from an intermediate point a distance from the ground terminal. The design has two advantages: the antenna is shorter and more compact, and the impedance matching can be tuned without changing the external dimensions. Above the ground surface is a thin, flat patch. This patch is the main radiation component of the antenna. The patch is short-circuited to a ground plane by a short, thin plate. Another plate called the feeding plate is used to energize the antenna. The location of the short plate and feeding plate has a specific effect on the antenna resonant frequency.

The basic parameters to adjust the PIFA design are the patch dimension (*L* and *W*), the height of the structure *h*, the width of the shorting pin W_{short} and the distance from the feeding to the pin. The sizes of *L*, *W,* and *h* are chosen to achieve a specific resonant frequency [11] as follows:

$$\left(L+W+h\right)\sqrt{\varepsilon_r} \cong \frac{\lambda}{4} \tag{7}$$

where ε_r is the permittivity of the substrate, λ is the free-space wavelength. Based on parametric studies when designing PIFA: PIFA's bandwidth increases with h (as in the case of conventional patch antennas) and the size of the resonant frequency-tuning patch (larger patch gives lower frequency). In addition, variations of the parameters are made to adjust the structure (position of shorting pin, position for feeding, the height of the air layer). The resonant frequency is approximated according to equation (8) in relation to the electrical length, while equation (9) is the relative permeability of the medium between the ground and the radiation plate. In addition, H is the height of the patch to the ground.

$$f_{r1} = \frac{c}{4\left(H+L_1+W_1\right)\sqrt{\varepsilon_{eff}}} \tag{8}$$

$$f_{r2} = \frac{c}{4\left(L_2+W_2\right)\sqrt{\varepsilon_{eff}}} \tag{9}$$

where ε_{eff} is the effective permittivity of the substrate, λ is the free-space wavelength, L_1 and W_1 is the length and width of the patch, L_2 and W_2 is the length and width of the slot inside the patch, *c* is the speed of light. In case there is an air layer between the patch and the ground plane, the effective permittivity ε_{eff} is calculated as follows:

$$\varepsilon_{eff} = \frac{\varepsilon_r \varepsilon_{air}\left(h_s+h_{air}\right)}{\varepsilon_r h_{air}+\varepsilon_{air} h_s} \tag{10}$$

where ε_r is the permittivity of the substrate, ε_{air} is the permittivity of the air, h_{air} is the height of the air between the two substrates, h_s is the thickness of the substrate. For low-cost fabrication, the substrate material chosen is FR4 with ε_r= 4.3 with a thickness of h_s= 1.6 mm, and the patch and ground plane are printed directly on the FR4 substrate with the height of the air between the two substrates is h_{air} = 5 mm. According to Equation (10), computed $\varepsilon_{eff} \approx 1.2256$. For the first band of f_{r1}= 2.45 GHz, the dimension $H+L_1+W_1 \approx$ 27.6533 mm. For the second band of f_{r2}=

5.8 GHz, the dimension $\left(L_2 + W_2\right)$ » 11.6812 mm. Besides, the input impedance for the antenna is 50Ω using the coaxial type.

4. OPTIMIZATION MODELLING FOR THE ULTRA WIDEBAND ANTENNA USING DIFFERENTIAL EVOLUTION ALGORITHM

The DE algorithm is a search algorithm that converges to an optimized value of the fitness function. Until any of the desired criteria is met, it successively produces a population of the physical dimensions. Figure 3 displays the flow diagram of the process using a different algorithm for such a semi-automated design of the antenna. In this antenna design, an optimization algorithm is coupled with simulation in CST Microwave Studio, and the steps are outlined below:

Step 1: Object components are created, and the ranges of frequency for impedance parameter simulations are defined in the .m file through Matlab.

Step 2: The proposed candidate solutions generated by the DE algorithm are transformed into an object and simulated in CST.

Step 3: The simulation is called for an evaluation of impedance parameters from the MATLAB.

Step 4: Once the simulation is over, the S_{11} parameter values are stored in the corresponding .txt file in a folder through text mode.

Step 5: Evaluation of S_{11} for fitness values in the procedure.

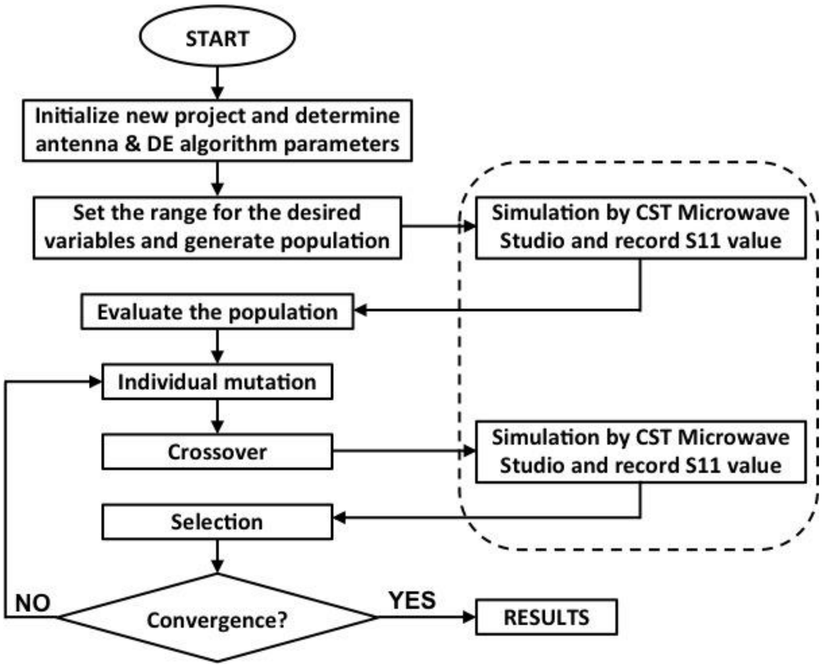

Figure 3.*Flow diagram of the differential evolution algorithm for semi-automatic antenna design.*

To obtain the desired performance, the first step of the process is to initialize the population of geometricalparameters of the structure. The performance of the PIFA structure corresponds to the given set *D* of geometrical parameters of the structure.

Here, we chose the set *D* as four parameters L_1, W_1, L_2, W_2. In the DE optimization process, *NP* population size is essential and is kept unchanged during the optimization process of the algorithm. The larger the *NP* value is, the better possible global solution can be observed, however, if the NP is too large, it will increase run time and reduce the efficiency of the algorithm. Therefore, it is crucial to select *NP* values with the appropriate population size. After a number of trials of population size change over 20 generations, the following chart is obtained in figure 4. From the chart in figure 4, we derive the *NP* value if it is too small ($NP<2D$), the probability of convergence is inferior and will increase gradually with the number of *NP* individuals. But when the *NP* reaches the value of about 4*D* to 7*D*, convergence ability does not change too much. Therefore, we can choose the *NP* value in the range from 4*D* to 7*D*. The number of *NP* will be selected after further investigation of the number of GEN generations.

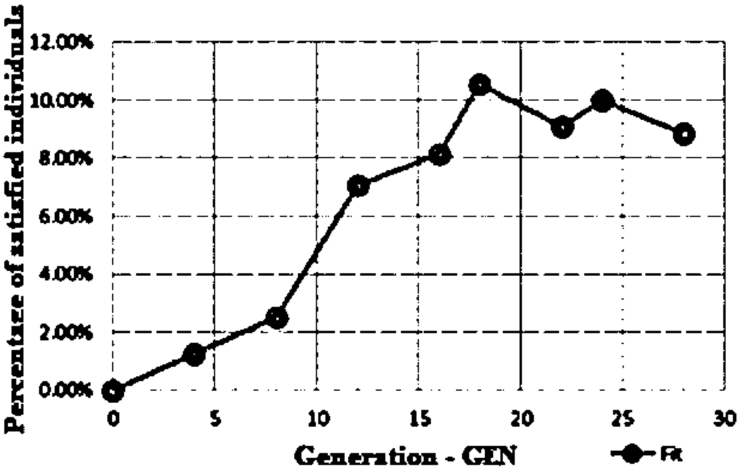

Figure 4. *Convergence characteristic of the population depending on the NP value.*

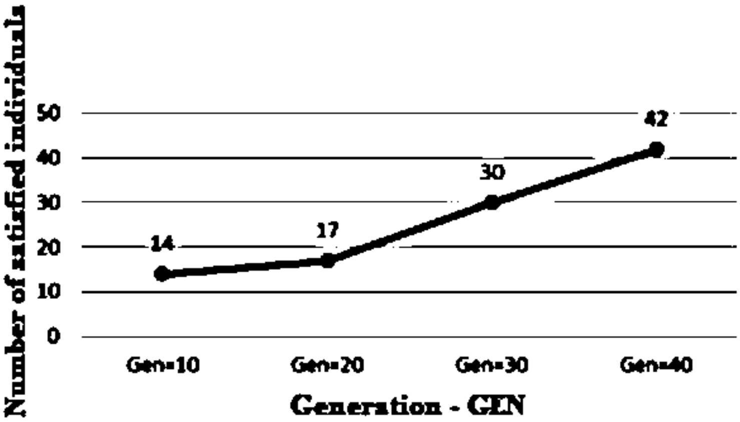

Figure 5. *Investigation chart of the dependence on the number of generation (GEN).*

In the next step, it is necessary to determine the GEN generation number of the algorithm. Thanks to the optimization iteration in Matlab software when running with CST Microwave Studio software, the trial run is chosen to 5000 runs. From this program, the number of GEN is investigated to find the optimal GEN and *NP* for the algorithm. We obtain the number of satisfied individuals versus the generation in the graph in figure 5. The number of satisfied individuals for GEN = 10, 20, 30, and 40 are 14, 17, 30, and 42, respectively.

From the number of eligible individuals obtained in the filtering process when verifying different cases of generation, we conducted the simulation of the reflection coefficient in order to find the optimal geometrical parameters. The results for these simulations are exhibited in figure 6. From the survey results extracted from figure 6, the number of generations after increasing from 10 to 40 demonstrates the higher convergence at both 2.45 GHz and 5.8 GHz. Moreover, the reflection coefficient value becomes much lower at GEN = 40 compared to GEN = 10. Table 1 summarizes the main properties of the reflection coefficient when increasing the generation number at two frequencies. With the statistics of the quality survey, it is shown that the more generations the S_{11} values of the good individuals decrease, which leads to lower the S_{11} values, and at the last generation, the quality of the individual reaches the most optimal value. That means the increasing number of generations will help increase the number of qualified individuals, and the quality of the following individuals becomes better. The number of generations (GEN) does not significantly determine the probability of convergence when the number of generations is not large. As in this case, the number of generations will be limited; hence we will choose more generations to increase the quality of the individuals. From the two surveys about NP and GEN, the values are chosen: NP = 18 and GEN = 25 (with NP * GEN <500). With this selection, the number of individuals is good enough for convergence. Besides, a large number of generations is found to increase the number and quality of individuals. This will be very beneficial in finding the best results.

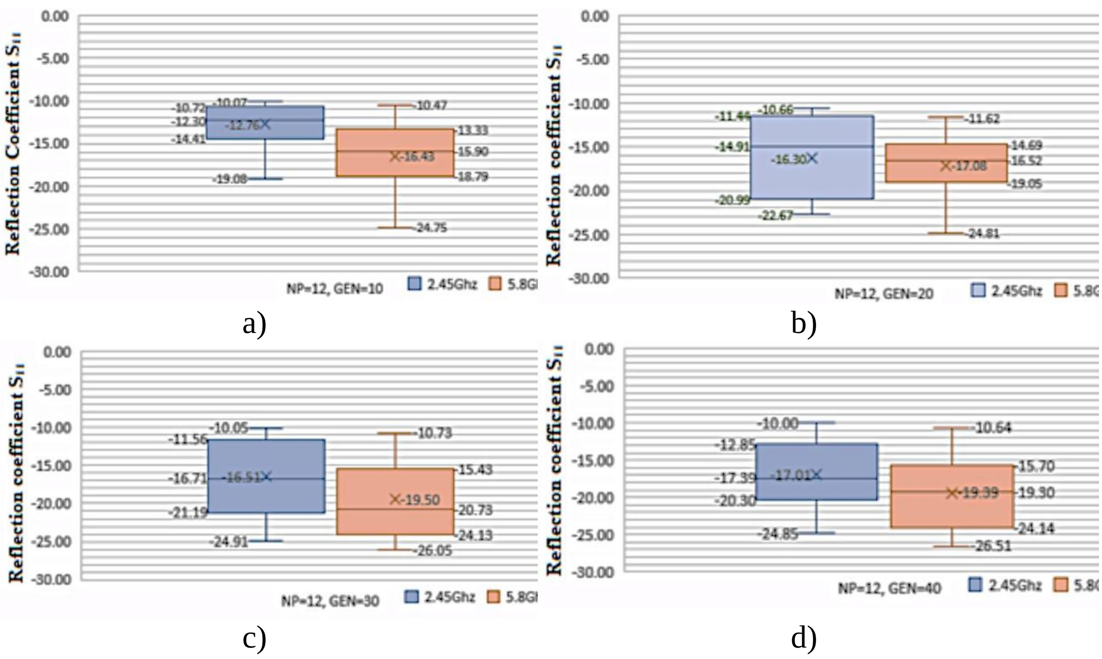

Figure 6. *Chart of individual quality survey.*

Table 1. *Individual quality survey on the generation number represented by reflection coefficient.*

NP	GEN	Reflection coefficient S_{11} at 2.45 GHz			Reflection coefficient S_{11} at 5.8 GHz		
		Distribution range	Median	Average	Distribution range	Median	Average
12	10	-10.72dB ÷ -14.41dB	-12.30dB	-12.76dB	-13.33dB ÷ -18.79dB	-15.90dB	-16.43dB
12	20	-11.44dB ÷ -20.99dB	-14.91dB	-16.30dB	-14.69dB ÷ -19.05dB	-16.52dB	-17.08dB
12	30	-11.56dB ÷ -21.19dB	-16.71dB	-16.51dB	-15.43dB ÷ -24.13dB	-20.73dB	-19.50dB
12	40	-12.85dB ÷ -20.30dB	-17.39dB	-17.01dB	-15.70dB ÷ -24.14dB	-19.39dB	-19.39dB

Differential evolution (DE) is one of the most popular evolutionary optimization techniques on continual domains based on simplicity, efficiency, and robustness. Differential amplification factor (F) and crossover probability constant (CR) allow the development of a new test element based on current and mutant factors. The CR constant controls and will determine the mutant component in each component of the current population. After testing with different values of F and CR within the range [0,1], there was no significant change to the final result. Because of the random nature of the rand() function, the exchange rate is only relevant. In this problem, the differential gain F and the CR probability coefficient are set to F = 0.8 and CR = 0.5 for the most suitable case.

After checking the quality survey, we will build an algorithm with four parameters: L_1, W_1, L_2, W_2. With the relative value calculations above according to the research in figure 5, we will embark on setting limits for those parameters. With the policy of designing a slot PIFA antenna oriented in the Oy axis, we will have the selectable values listed in table 2.

Table 2. *The setting parameters for optimization of the PIFA antenna.*

Parameters	L_1	W_1	L_2	W_2
Range (mm)	15 ÷ 20	10 ÷ 15	6 ÷ 7	4.5 ÷ 6

The purpose of choosing a relatively wide range of tuning, as shown in Table 2, is because of the interaction and mutual coupling of the inner radiation plate (5.8 GHz) and the outer bounding radiation patch of the frequency of 2.45 GHz. Therefore, it is advisable to choose a wide range so that there are many experimental choices that produce consistent results.

5. RESULTS AND DISCUSSION

To investigate the impact of the DE algorithm, we implemented the semi-automatic antenna design process by combining simulation on CST Microwave Studio software and algorithm program on Matlab. We conducted two tests, of which the first one was from the individual quality survey process; we narrowed the limit of the parameters to be able to have a better individual set. In the second test, we experimented with conditional constraints for narrowing parameters to be more specific. After the first test, we obtained four graphs in figure 7 showing the distribution of parameters L_1, W_1, L_2, W_2 of the individuals who met the above requirements.

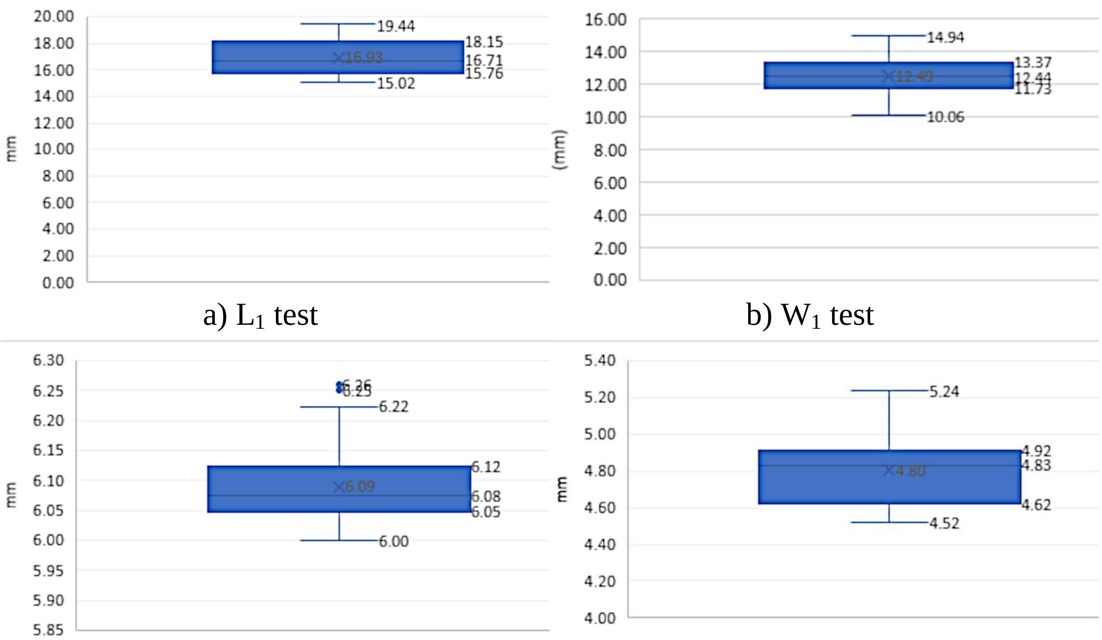

a) L_1 test b) W_1 test

c) L_2 test d) W_2 test

Figure 7. *Geometrical parameter distribution using the DE algorithm.*

According to figure 7a, L_1 is distributed mainly in the range of 15.76mm to 18.15mm and concentrates more values in the range from 15.76mm to 16.71mm. According to figure 7b, L1 is distributed mainly in the range of 11.73mm to 13.37mm and concentrates more values in the range of 11.73mm to 12.44mm. According to figure 7c, L_2 is distributed mainly in the range of 6.05mm to 6.12mm and concentrates more values in the range from 6.05mm to 6.08mm. In figure 7d, W_2 is distributed mainly in the range of 4.62mm to 4.92mm and concentrates more values in the range from 4.62 mm to 4.83mm. From these distributions, we continue to test a second time with the constraint for narrower parameters, as shown in Table 3.

Table 3. *The geometrical parameters for the second optimization of the PIFA antenna.*

Parameters	L'_1	W'_1	L'_2	W'_2
Range (mm)	15.5 ÷ 18.5	11.5 ÷ 13.5	6 ÷ 6.15	4.5 ÷ 5

At this second test, the number of qualified individuals reached 429/450 individuals. From the initial population, individuals are gradually replaced after each generation, and after GEN = 25 generations, the best offspring of each original is valued as table 4 and table 5.

Table 4. *The obtained reflection coefficient after each trial of NP value.*

NP	*1*	*2*	*3*	*4*	*5*	*6*	*7*	*8*	*9*
S_{11} at 2.45 GHz (dB)	-15.05	-18.28	-23.93	-23.28	-23.83	-22.73	-23.73	-24.10	-25.03
S_{11} at 5.8 GHz (dB)	-24.76	-24.45	-24.63	-23.76	-17.81	-19.56	-23.71	-24.10	-17.04
NP	***10***	***11***	***12***	***13***	***14***	***15***	***16***	***17***	***18***
S_{11} at 2.45 GHz (dB)	-23.41	-23.55	-21.09	-14.51	-23.79	-23.39	-23.65	-23.81	-25.18
S_{11} at 5.8 GHz (dB)	-21.04	-24.62	-24.62	-24.62	-24.13	-22.47	-20.01	-23.87	-17.55

Table 5. *The obtained geometrical parameters after each trial of NP value.*

NP	*1*	*2*	*3*	*4*	*5*	*6*	*7*	*8*	*9*
L_1	6.13	6.14	6.09	6.08	6.05	6.07	6.00	6.13	6.04
W_1	4.63	4.58	4.68	4.69	4.92	4.85	4.93	4.58	4.65
L_2	17.15	17.29	16.40	16.08	16.27	16.38	16.60	16.66	16.88
W_2	13.30	12.22	12.44	12.96	12.79	13.06	12.36	12.35	11.57
NP	***10***	***11***	***12***	***13***	***14***	***15***	***16***	***17***	***18***
L_1	6.05	6.11	6.11	6.07	6.06	6.02	6.05	6.02	6.13
W_1	4.88	4.64	4.66	4.75	4.77	4.82	4.71	4.86	4.71
L_2	16.48	16.41	16.73	17.22	16.64	16.16	16.49	16.62	16.92
W_2	12.66	12.30	12.75	13.32	12.34	13.23	12.59	11.88	11.59

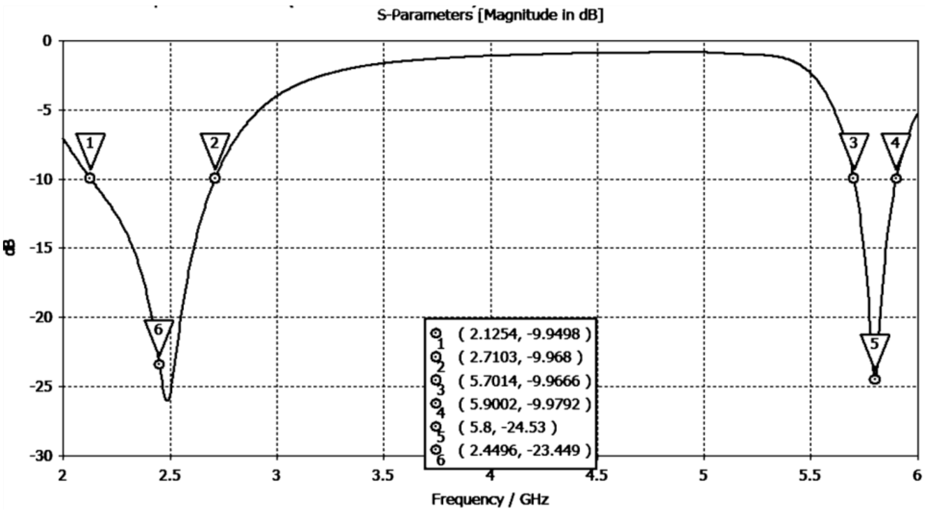

Figure 8. *The reflection coefficient of the selected parameters.*

To select the appropriate result, based on the returned S_{11} value set in table 4, we select the appropriate set (obtained S_{11} at 2.45GHz = -23.93dB and at 5.8GHz = -24.63dB) to operate at the frequency of 2.45GHz and 5.8GHz are L_1 = 16.40mm, W_1 = 12.44mm, L_2 = 6.09mm, W_2 = 4.68mm. With the parameters found, on CST software, we get the results as shown in figure 8.

The result shows that the antenna has two bandwidths for the proposed antenna at 2.45 GHz and at 5.8 GHz of 590 MHz and 200 MHz, respectively. Although the lowest peak of the S_{11} line is not at 2.45 GHz due to the way of targeting the best results at 5.8 GHz (because at this frequency, the parameter value is very small and affects the resonant frequency, it is preferable to choose to have good results at both frequencies), thus, the algorithm has also shown a good result at this frequency, and precisely the lowest point of S11 is frequency 5.8 GHz. With the goal of selecting S_{11} at the frequency of 2.45 GHz to be the best, we also get the results as shown in figure 8 only through one test. At 2.45 GHz, S_{11} reaches the smallest value at -27.15dB with a bandwidth of 530 MHz and at 5.8 GHz frequency of -20.3 GHz with a bandwidth of 178 MHz. Consequently, for each manufacturing purpose, we can change the target of selecting the best individual to achieve the request. With the implementation of various mutation strategies (DE/rand/1, DE/best/1, DE/current-to-rest/1, RDE) mentioned in section 2 in the same case with parameters of the first test, we get the result in figure 9.

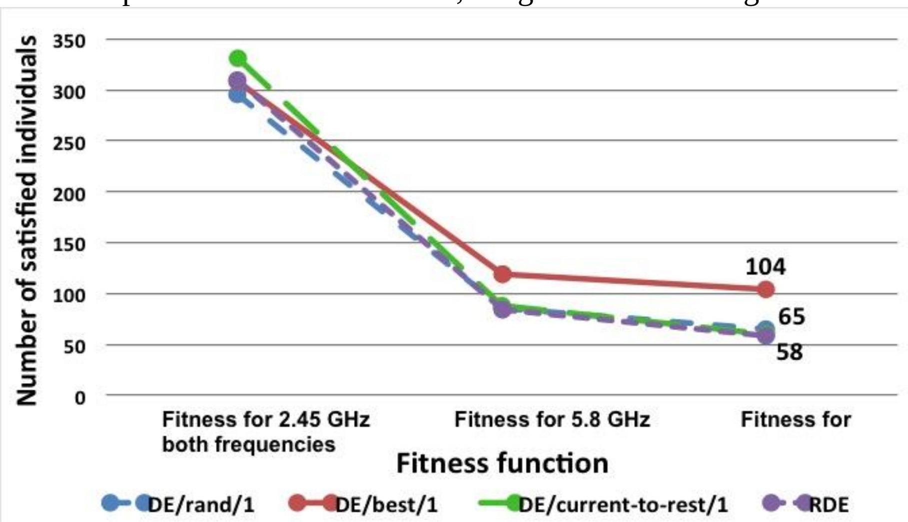

Figure 9.*Strategic efficiency chart.*

Figure 9 clearly shows the effectiveness of the DE/best/1 strategy when applied to this PIFA antenna design with the number of individuals meeting the requirements of up to 104/450 individuals, superior to those of other strategies when they are only between 58 and 65 individuals. At the frequency of 5.8 GHz, this strategy is also clearly effective. Hence, with a useful parameter limit constraint, the DE/best/1 strategy will prove very useful. With the parameters limited to the second test, the results with the DE/best/1 strategy yielded an absolute number of 100%. With the parameters selected above, we perform antenna simulations and produce prototypes for measurement from design (figure 10). Simulation and measurement results are shown in figure 11.

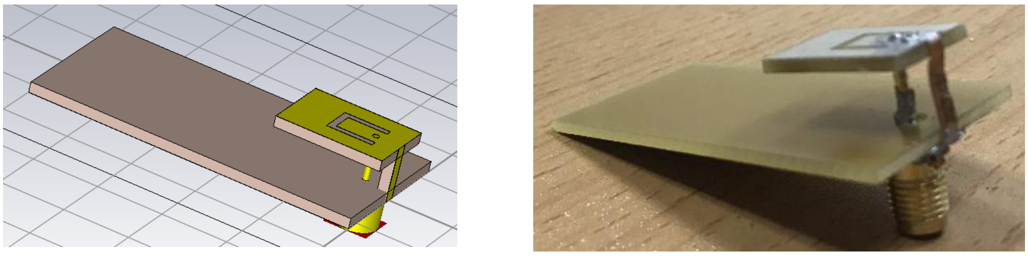

a) b)

Figure 10. *a) PIFA simulated structure; b) Photo of fabricated PIFA.*

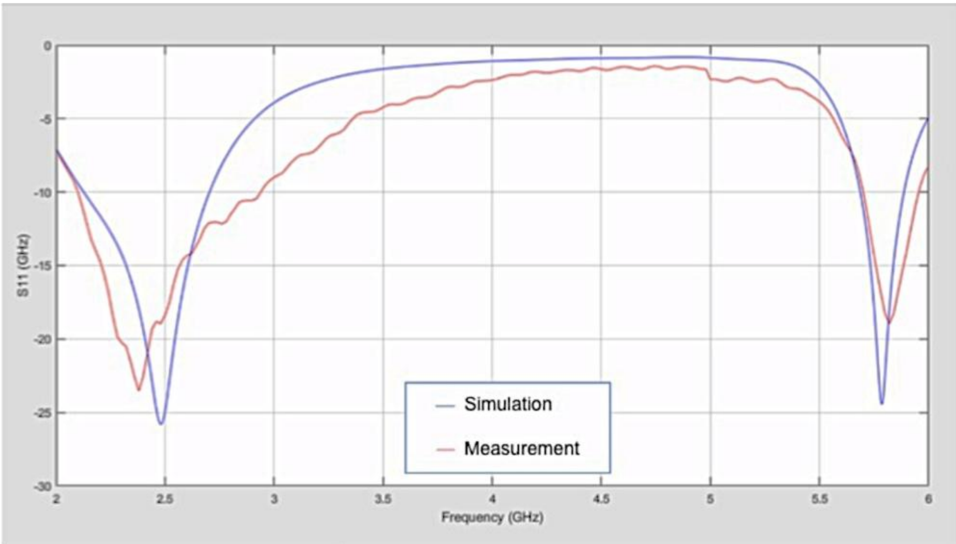

Figure 11. *Simulated and measured reflection coefficient of the proposed PIFA.*

Through figure 11, it can be seen that thesimulation and measurement results deflect but not significantlydue to the fabrication process and the material quality. However, the antenna can still work well in reality in both frequency bands of 2.45 GHz and 5.8 GHz with a reflection coefficient of approximately -19.00dB and -18.23dB, respectively. When measured in reality, the bandwidth at 2.45 GHz and 5.8 GHz are more significant than the simulated bandwidth in CST software. They are 780 MHz (2.15 GHz to 2.93 GHz) at 2.45 GHz and 240 MHz (5.71 GHz to 5.95 GHz) at 5.8 GHz. The radiation pattern is also investigated at two frequencies (figure 12). At the frequency of 2.45GHz, the radiation pattern of the antenna is directed towards the upper surface perpendicular to the antenna plane with quite large gain. The results show that the gain in the frequency of 2.45GHz is 3.091dBi, indicating that the received power or the output from the antenna will be 3.091 dB (nearly double) of the received input power. At 5.8GHz, the antenna radiation is towards the lower part of the ground. The orientation at this frequency is very small because the radiation generated at 5.8 GHz is intensely absorbed by the FR4 substrate. The antenna gain is only 1,026dBi, relatively low compared to the average gain of an omnidirectional antenna. At 5.8 GHz, the main beam has a resonance angle of 52.7 degrees and the strongest resonance at an angle of 65 degrees. The side beam of the antenna causes interference and radiates in all directions, showing the average level of antenna directivity at this frequency.

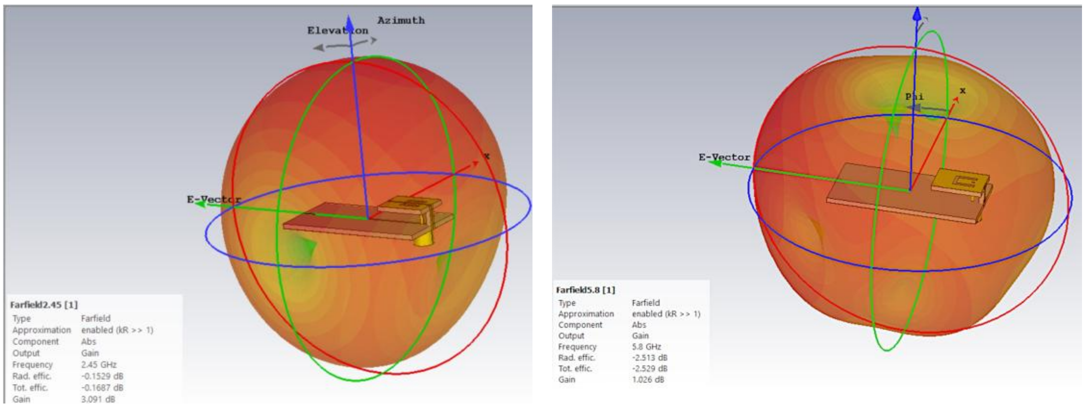

a) b)

Figure 12. *Radiation pattern of PIFA at: a) 2.45 GHz; b) 5.8 GHz.*

To explain for PIFA's radiation properties, a graph of surface current in Figure 13 will clearly show this property.

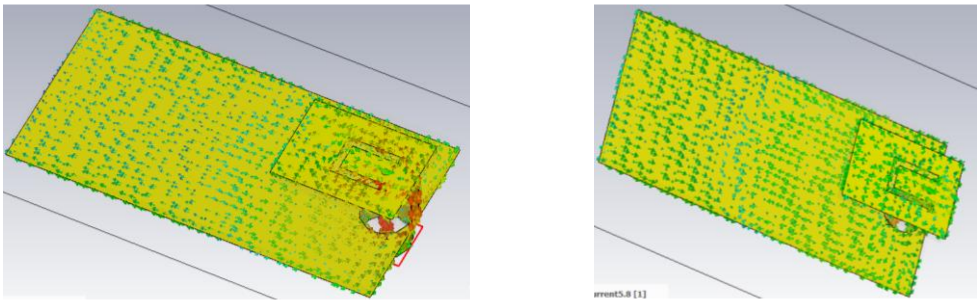

a) b)

Figure 13. *Surface current pattern of PIFA at: a) 2.45 GHz; b) 5.8 GHz.*

In figure 13, at 2.45GHz, the current flows from the coaxial cable power supply to the upper reflector surface and comes from the short circuit of the current. The current flows along the plane of the radiation plate but concentrates at the edge of the groove, essentially in line with theoretical calculations. The total energy supplied to the antenna is concentrated towards the radiation plate, and therefore, the orientation of the radiation plate at this frequency is in the direction perpendicular to the reflector plate and is stronger at the plane towards the reflector plate. At 5.8GHz, because the radiated part of this frequency is made up mainly of the groove, the current from the power supply is the primary energy source for the radiation of the antenna at this frequency. The electric current taken from the short circuit is almost negligible. In addition, due to the small size of the groove, while the thickness of the FR4 range is quite significant, the energy lost due to the substrate is significant. Therefore, the orientation at 5.8 GHz is small. In further research, this structure also needs to be further improved to increase the antenna's ability to radiate at this frequency.

6. CONCLUSION

In this paper, we described our work in semi-automated, designing a dual-band PIFA antenna. The purpose of the work is to find the optimal geometrical parameters by making use of an evolutionary algorithm. The antenna dimensions are optimized by applying different generation of crossover and mutation to find the most suitable fitness value. In order to validate the employment capability,the antenna prototype is fabricated and measured. The antenna can operate well in the intended frequency range with the tiny deflection between the simulation and the measurement. It proves that the DE algorithm can perform a significant impact on the antenna design problem.

Acknowledgment: *This research is funded by the Hanoi University of Science and Technology (HUST) under project number T2020-PC-019.*

REFERENCES

[1]. N. Elamin, and R. Tharek, "*Multiband Antenna for Modern Wireless Communication.*", Wideband, Multiband, and Smart Reconfigurable Antennas for Modern Wireless Communications. IGI Global, pp. 123-144, 2016.

[2]. H. W. Hsieh, Y. C. Lee, K. K. Tiong, and J. S. Sun. "*Design of a multiband antenna for mobile handset operations*.", IEEE Antennas and Wireless Propagation Letters, vol.8, pp. 200-203, 2008.

[3]. Y. L. Kuo, and K. L. Wong, "*Printed double-T monopole antenna for 2.4/5.2 GHz dual-band WLAN operations.*", IEEE Transactions on Antennas and Propagation, vol. 51, no. 9, pp. 2187-2192, 2003.

[4]. D. Mandal, and S. S. Pattnaik, "*Wide CPW-fed multiband wearable monopole antenna with extended grounds for GSM/WLAN/WiMAX applications*", International Journal of Antennas and Propagation, 2019..

[5]. M. C. Chang, and W. C. Weng, "*A dual-band printed dipole slot antenna for 2.4/5.2 GHz WLAN applications.*", IEEE International Symposium on Antennas and Propagation (APS/URSI), 2011.

[6]. A.S. Al-Hiti, *"Design of rectangular microstrip patch antenna for WLAN and WiMAX applications"*, ARPN Journal of Engineering and Applied Sciences, vol. 14, no. 2, pp. 433-438, January 2019.

[7]. T. S. Ooi, S. K. A. Rahim, and B. P. Koh, "*2.45 GHz and 5.8 GHz compact dual-band circularly polarized patch antenna.*", Journal of Electromagnetic Waves and Applications, vol. 24, no. 11-12, pp. 1473-1482, 2010.

[8]. C. C. Lin, E. Z. Yu, and C. Y. Huang, "*Dual-band rhombus slot antenna fed by CPW for WLAN applications*.", IEEE Antennas and Wireless Propagation Letters, vol. 11, pp. 362-364, 2012.

[9]. R. K. Raj, M. Joseph, B. Paul, and P. Mohanan, "*Compact planar multiband antenna for GPS, DCS, 2.4/5.8 GHz WLAN applications*.", Electronics Letters, vol. 41, no. 6, pp. 290-291, 2005.

[10]. A. El Yousfi, A. Es-Salhi, A. Lamkaddem, O. El Mrabet, M. Aznabet, M. and M.A. Ennasar, "*A dual band inverted L monopole antenna based on Complemenatry Split ring Resonator for RFID applications*", International Conference on Wireless Technologies, Embedded and Intelligent Systems (WITS), pp. 1-3, April 2019.

[11]. H. T. Chattha, M. K. Ishfaq, Y. Saleem, Y. Huang, and S. J. Boyes, "*Band-notched ultrawide band planar inverted-F antenna*.", International Journal of

Antennas and Propagation, 2012.

[12].S. Chamaani, S. A. Mirtaheri, "*Planar UWB monopole antenna optimization to enhance time-domain characteristics using PSO*.", AEU-International Journal of Electronics and Communications, vol. 64, no. 4, pp. 351-359, 2010.

[13]. A. Deb, J. S. Roy, and B. Gupta, "*Design of a probe-fed microstrip antenna using differential evolution algorithm*.", 4th IEEE International Symposium on Microwave, Antenna, Propagation and EMC Technologies for Wireless Communications, pp. 46-49, 2011.

[14].R. Storn R. and K. Price, "*Differential evolution - a simple and efficient heuristic for global optimization over continuous spaces*", Journal of Global Optimization, vol. 11, no. 4, 341-359, 1997.

[15].K. Price, R. M. Storn and J. A. Lampinen, "*Differential Evolution - A Practical Approach to Global Optimization*", Springer, 2005.

[16].S. Das and P. Suganthan, "*Differential evolution: A survey of the state-of-the-art. IEEE Transactions on Evolutionary Computation*", vol. 15, no. 1, pp. 4-31, 2011.

TÓM TẮT

PHƯƠNG PHÁP THIẾT KẾ BÁN TỰ ĐỘNG VÀ TỐI ƯU HÓA CHO ĂNG TEN BĂNG TẦN KÉP CẤP NGUỒN CÁP ĐỒNG TRỤC SỬ DỤNG THUẬT TOÁN TIẾN HÓA VI PHÂN CHO ỨNG DỤNG WLAN

Thiết kế ăng-ten truyền thống sử dụng các bước riêng biệt bằng tay để tạo và tối ưu hóa cấu trúc ăng-ten. Cách tiếp cận này tốn cả thời gian và công sức, đặc biệt là khi một cấu trúc ăng ten phức tạp được yêu cầu. Thuật toán tiến hóa ra đời như một phương pháp thay thế tiềm năng để xây dựng mô hình ăng ten cũng như tối ưu hóa cấu trúc để tuân thủ các yêu cầu thiết kế. Trong bài báo này, chúng tôi đề xuất một phương pháp xác định mô hình thay thế và kích thước của ăng ten vá siêu băng rộng bằng thuật toán tiến hóa vi phân. Ăng-ten này được chế tạo để hoạt động ở dải tần 2,45 GHz và 5,8 GHz cho các ứng dụng WLAN. Thông qua việc đánh giá độ phản xạ và khảo sát mô hình có được, phương pháp này nhanh hơn và hiệu quả hơn khi tối ưu các kích thước. Thuật toán được nghiên cứu với các chiến lược khác nhau để phát hiện chiến lược tốt nhất khi áp dụng tiến hóa vi phân.

Từ khóa: Thuật toán tiến hóa; Tiến hóa vi phân; Ăng ten đa băng tần; Nguồn cấp đồng trục.

Received 26th May 2020
Revised 13thNovember 2020
Accepted16th November 2020

Author affiliations:

Hanoi University of Science and Technology.
*Corresponding author: huong.nguyenthanh3@hust.edu.vn.